Review

Development and Application of Surface-Enhanced Raman Scattering (SERS)

Zhenkai Huang , Jianping Peng , Liguo Xu , Peijiang Liu *

Posted Date: 22 July 2024

doi: 10.20944/preprints202407.1632.v1

Keywords: SERS, application, interaction

Review

Development and Application of Surface-Enhanced Raman Scattering (SERS)

Zhenkai Huang 1, Jianping Peng 2, Liguo Xu 3 and Peijiang Liu 4,*

1 School of Materials and Energy, Foshan University, Foshan 528000, China; hzk@fosu.edu.cn
2 School of Environmental and Chemical Engineering, Foshan University, Foshan 528000, China; pjp@fosu.edu.cn
3 College of Light Chemical Industry and Materials Engineering, Shunde Polytechnic, Foshan, 528333, China; 21099@sdpt.edu.cn
4 Reliability Physics and Application Technology of Electronic Component Key Laboratory, the 5th Electronics Research Institute of the Ministry of Industry and Information Technology, Guangzhou 510610, China
* Correspondence: cz2343222@163.com

Abstract: Since the discovery of the phenomenon of surface-enhanced Raman scattering (SERS), it has gradually become an important tool for the analysis of material compositions and structures. The applications of SERS have been expanded from the fields of environmental and materials science to biomedicine, due to the extremely high sensitivity and non-destructiveness of SERS-based analytical technology that even allows single molecule detection. This article provides a comprehensive overview of Surface-Enhanced Raman Scattering (SERS) phenomenon. The content is divided into several main sections: basic principles and the significance of Raman spectroscopy; historical advancements and technological progress in SERS, as well as various practical applications across different fields. We also discussed how electromagnetic fields contribute to the SERS effect, the role of chemical interactions in enhancing Raman signals, modeling and computational approaches to understand and predict SERS effects.

Keywords: SERS; application; interaction

1 Introduction to Raman Scattering Spectroscopy

In 1923, a German physicist, Smekal, proposed the existence of intrinsic inelastic scattering of light [1]. In 1928, two Indian physicists, Raman and Krishnan, using mercury lamps, prisms, and photographic substrates as experimental tools, discovered for the first time the phenomenon of inelastic scattering of liquid benzene, and called this inelastic scattering produced by the interaction of a vibrating molecule with incident light Raman scattering [2]. Raman scattering. Raman scattering is a scattering phenomenon that can be used to detect molecular vibrations [3,4]. The As shown in Figure 1 shown, when a sample is irradiated by a monochromatic laser beam, the sample molecules interact with the laser beam and emit scattered light in all directions. Most of the incident light frequency is equal to the scattered light frequency and is called Rayleigh scattering, while a portion of the scattered light that is different from the incident light frequency is called Raman scattering. In this case, Stokes lines appear when the frequency of the scattered radiation is lower than the frequency of the incident light, and anti-Stokes lines appear when the frequency of the scattered radiation is higher than the frequency of the incident radiation [5,6]. In Raman scattering, photons change momentum while exchanging energy with molecules. Therefore, parameters such as the intensity, number and displacement of peaks in the Raman spectrum contain information about the structure and composition of the excited molecules. Raman scattering is prevalent in a wide variety of substances, including gases, liquid and solids. Each different substance has its own characteristic

 doi:10.20944/preprints202407.1632.v1

"fingerprint" Raman spectrum, so that different substances can be identified and characterized using Raman spectroscopy.

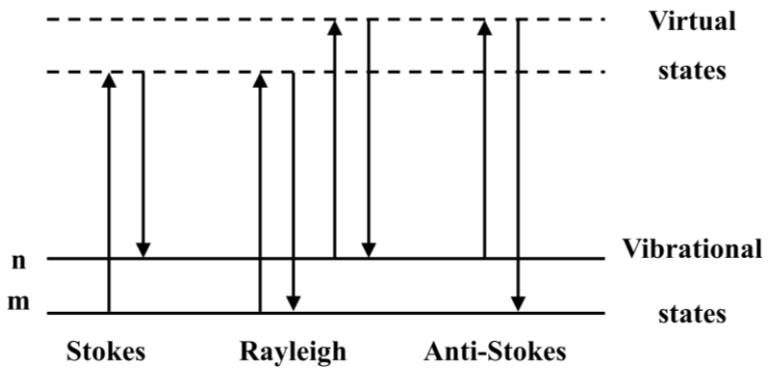

Figure 1. Illustration of Rayleigh and Raman scattering [7].

Since its discovery, Raman spectroscopy has quickly become a powerful analytical technique for detecting chemical compositions as well as other important information [8,9]. Raman spectroscopy has significant advantages over infrared spectroscopy. Raman spectroscopy has significant advantages over infrared spectroscopy, one of which is that it is less affected by the sample's environment, such as ambient carbon dioxide and water, so it has a wider range of applications. However, the sensitivity of Raman scattering is very low and the detection signal is very unstable, which severely limits the practical application of Raman spectroscopy [10]. The sensitivity of Raman scattering is very low and the detection signal is very unstable, which seriously limits the practical application of Raman spectroscopy. In the early development of Raman scattering technology, mercury lamp was used as a new excitation light source for Raman scattering. Until after 1960, laser was developed as the excitation light source. Lasers have the characteristics of high power, high energy, excellent monochromaticity, and polarizability, which have led to the rapid development of Raman scattering spectroscopy, and have been widely used in various fields [11].

2. Development of SERS Technology

Although Raman spectroscopy has many advantages, however, the Raman scattering signal is so weak that it is difficult to be detected by conventional laser Raman spectrometers. It was not until the 1970s that Fleischmann et al. at the University of Southampton in the UK [12]. accidentally discovered the ultra-intense Raman spectrum of pyridine on the surface of a rough silver electrode and attributed this phenomenon to the enhancement effect of the rough silver surface. Subsequently, Jeanmaire and Van Duyne et al [13]. and Albrecht et al [14]. discovered and verified the existence of this phenomenon at, respectively. For the reason of this phenomenon, they suggested that the enhancement of the ultra-strong Raman signal is not only due to the increase of the number of adsorbed molecules on the surface, but also due to the existence of some kind of Raman scattering enhancement effect of the adsorbed molecules on the substrate surface. However, this work on Raman surface enhancement effects went through a lengthy review process before it was published. Shortly thereafter, the American Chemical Society paid attention to this phenomenon and explained it as a resonance-like Raman effect, i.e., the Surface-enhanced Raman Scattering (SERS) effect. Specifically, the SERS phenomenon refers to the amplification and enhancement of Raman scattering signals of organic molecules when they are adsorbed on the surface of some materials. In particularly, when adsorbed on the surface of nanoparticles, the Raman signals of organic molecules can even be enhanced by tens of billions of times, which completely makes up for the shortcomings of the low sensitivity of Raman scattering spectroscopy, and thus has a huge potential for development in the areas of single-molecule detection and probing applications. Therefore, the mechanism of SERS has become an exciting scientific phenomenon and has gradually become a research hotspot in related fields.

 doi:10.20944/preprints202407.1632.v1

3. Theoretical Mechanisms for the Emergence of the SERS Phenomenon

The study of the mechanism of the SERS phenomenon is important for the development of SERS, but the results of this study are still inconclusive. Theoretical simulations have also been used to study the mechanism of the SERS phenomenon, and the theoretical modeling of SERS has a long history and has undergone many modifications [15]. Theoretical modeling has also been used to study the mechanism of the SERS phenomenon. After a large number of experimental verification, researchers in the field of SERS have reached a consensus that the Raman enhancement factor is caused by the electromagnetic enhancement effect of plasma excitation of electrons in metal particles and the chemical enhancement effect of the electron transfer of the probe molecules in metal particles, among which the electromagnetic enhancement effect is considered to be the main factor in the generation of SERS, and the factors affecting the electromagnetic enhancement are mainly related to the following points Related:

(1) Relating to the material of the SERS substrate The SERS substrate refers to the material that provides the plasma resonance that produces the SERS effect. This generally refers to metallic materials such as gold, silver, copper, and aluminum, as well as materials that are being investigated, such as electrolytes and semiconductor materials.

(2) Related to "hot spots", the electromagnetic enhancement on the surface of the SERS substrate is not uniform, and the enhancement mainly occurs in very small and narrow areas, i.e. "hot spots". From the physical structure, the signal amplification is more efficient at the sharp tip and the gap between the nanoparticles.

(3) Distance dependent. As the distance from the surface increases, the Raman signal intensity decreases very rapidly, so the probe molecules need to be kept within 10 nm of the substrate surface during testing to better utilize the plasma effect.

The different mechanisms are described separately next.

3.1. Electromagnetic Enhancement Mechanism

The electromagnetic enhancement effect is generally produced on the surface of special nanostructures, and the effect is caused by the collective vibration of conduction electrons in metallic nanoparticles, and the vibration of the conduction electrons causes the enhancement of the localized electromagnetic field and thus greatly enhances the intensity of the Raman signal of molecules within the range [17,18]. This effect is caused by the collective vibrations of the conduction electrons in the metal nanoparticles. The principle of the electromagnetic enhancement effect is shown in Figure 2. The principle of electromagnetic enhancement is shown in Figure 2 [16]. The interaction between the incident photon beam with wavelength λ_0 and the nanostructures will lead to the localized enhancement of the incident field E_0, and the molecules within the radiation range of the nanoparticles will also feel the enhanced electric field strength E_{LOS}, where $E_{LOS} = M_{loc}(\lambda_0)E_0$. ($M_{loc}(\lambda_0)$ is the EF of the localized electric field). Upon excitation by the enhanced electric field, these molecules scatter a Raman signal at a wavelength of λ_R ($\lambda_R \neq \lambda_0$), and the scattered field E_{scat} radiated by photons at a wavelength of λ_R is also enhanced compared to the scattered field of the molecule in the absence of the nanostructure present ($E_{scat} = \alpha E_{LOS} = \alpha M_{loc}(\lambda_0)E_0$). The interaction between the scattered field E_{scat} and the nanoparticle causes it to be enhanced again, and the field is radiatively enhanced again as $E_{SERS} = M_{rad}(\lambda_R)E_{scat} = M_{rad}(\lambda_0)\alpha E_{LOC} = \alpha M_{loc}(\lambda_0)M_{rad}(\lambda_R)E_0$, so that the intensity of the Raman signal of the molecule in the range of the nanoparticle's action is proportional to the intensity of the Raman signal of the molecule in the range of the nanoparticle's action. Since the field enhancement at a particular incident wavelength can occur twice consecutively, the molecule is finally subjected to a total electric field enhancement of $|E|^4_{SERS}$, making the SERS effect significant.

 doi:10.20944/preprints202407.1632.v1

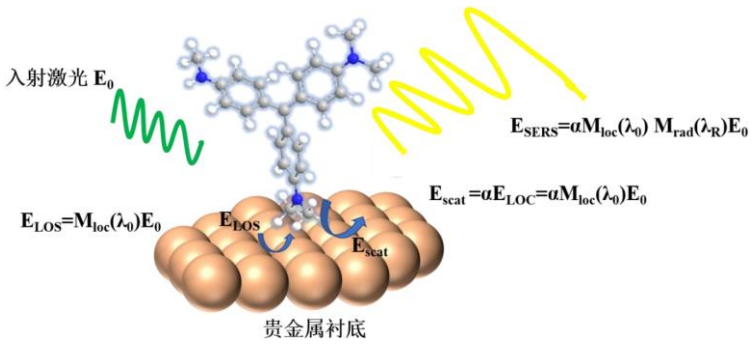

Figure 2. The schematic diagram of SERS electromagnetic enhancement [16].

However, this electromagnetic enhancement has limitations, mainly in the fact that its enhancement decreases rapidly with increasing distance between the adsorbed molecules and the metal particles (in the ratio of 1/r3 of the distance r from the metal surface), and the range of the effect is generally from 10 to 100 Å, which is a long-range enhancement effect, which makes SERS a surface-sensitive technique [19–21]. This makes SERS a surface sensitive technique.

Surface Plasmon Resonance (SPR) causes molecules adsorbed on the surface of nanoparticles to experience an enhancement of the local electric field. Although the increase in the local electric field is generally insignificant, the intensity of inelastically scattered light is enhanced to the fourth power of the original intensity, resulting in a very significant SERS effect. SPR is a phenomenon that occurs when free electrons on the surface of a metallic nanoparticle are excited by electromagnetic wave irradiation and then undergo a collective oscillation phenomenon that generates an electromagnetic wave, and when the frequency of the incident electromagnetic wave is the same as the intrinsic frequency of the oscillating free electrons, as shown in Figure 3 [22]. The localized surface plasma resonance (LSPR) Localized Surface Plasmon Resonance (LSPR) refers to the surface plasmon resonance phenomenon confined to a small range of the metal surface, and generally, the surface of precious metals can produce the SERS effect with an EF of 106 ~1011. The surface plasmon resonance phenomenon is reflected in the spectral characteristics of the precious metal nanoparticles, mainly in the absorption bands generated in the visible range. The incident laser frequency determines the intensity of the plasma resonance generated on the surface of the noble metal nanoparticles. When the Raman signal frequency slightly deviates from the frequency of the incident light, and both the Raman signal and the incident laser frequency are located near the plasma resonance frequency, the resonance occurs at this time, and produces an enhancement of the $|E|^4_{SERS}$; when the Raman scattering frequency deviates a lot from the incident laser frequency, the incident light and the Raman signal can not be simultaneously resonated with the plasma, and the electrostatic force is increased. When the Raman scattering frequency deviates much from the incident laser frequency, the incident light and Raman signal cannot resonate with the plasma at the same time, and the electric field enhancement effect is greatly reduced. In addition, when Raman scattering occurs, the plasma oscillation direction must be perpendicular to the surface of the substrate, so it is generally necessary to use a curved or rough surface to generate localized collective oscillations, and nanoparticles with a size of 100 nm or less as the enhancement of the substrate is a very good choice [23]. The size of nanoparticles within 100 nm is a very good choice as the enhancement substrate.

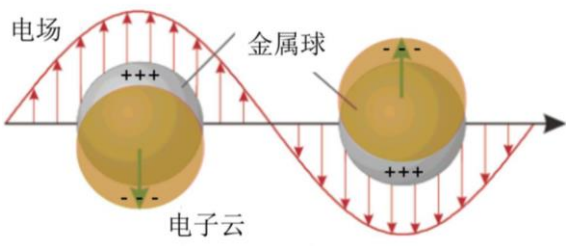

 doi:10.20944/preprints202407.1632.v1

Figure 3. Schematic of plasmon oscillation for a metal nanosphere [22].

Au, Ag, and Cu are the most widely used noble metal SERS substrates, and their corresponding LSPR peaks are all in the visible region, but are different from each other, with peak positions of 2.1 eV, 2.3 eV, and 3.5 eV, respectively (see e.g. Figure 4). The positions of the LSPR peaks for the same noble metal SERS substrates are also not completely fixed. This is because the location where the LSPR peaks appear is not only affected by the metal type, but also related to the structure, size, shape, aggregation state and dielectric environment of the metal [24]. Therefore, the LSPR peaks of precious metals are generally adjusted by regulating various parameters of the metal, such as the ratio between the components, and the position of the LSPR peaks is also not fixed [25]. Therefore, it is common to adjust the position of the LSPR peaks of precious metals to the vicinity of a specific incident wavelength to maximize the enhancement of the electromagnetic field and the strongest SERS effect.

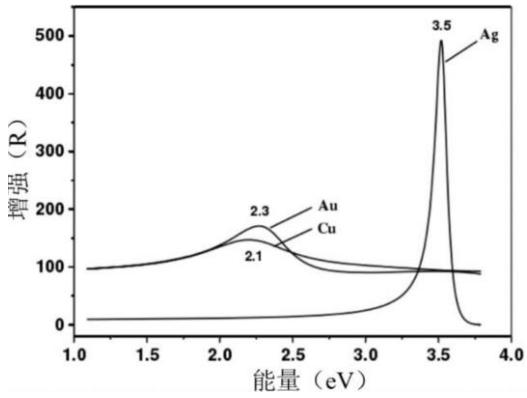

Figure 4. The LSPR peak of noble metals Ag, Cu and Au [26].

In addition, “hotspots” are specialized regions of highly spatially localized electric fields that are greatly enhanced by LSPR [27]. In addition, “hotspots” are special regions of strong spatial localization with greatly enhanced local electric fields caused by LSPR. The “hotspot” effect usually occurs at connections or gaps between noble metal nanoparticles, or in highly curved regions with a small radius of curvature, such as corners or tips of nanostructures (the “lightning rod” effect), or at topographies with nanometer-scale roughness, etc [28–30]. The “hotspots” are the areas where the nanostructures are highly curved. SERS EFs of up to 1015 at “hot spots” make single-molecule detection possible [31,32]. However, the “hotspots” have a high SERS EF of up to 10 However, there is a very clear spatial limitation at the “hotspots” [33]. However, there is a very obvious spatial limitation at the “hotspot”, where only the Raman signals of molecules falling within the “hotspot” region on the surface of the noble metal substrate are significantly enhanced, while the Raman signals of other molecules falling outside the “hotspot” range are not significantly enhanced. Due to the uneven spatial distribution of the “hot spots”, the Raman signals of molecules usually change with the location. Examining the distribution of the SERS EF of the silver film on the nanoparticle surface, it was found that the probe molecules falling within the “hotspot” range with an EF greater than 109 (less than 0.01% of the total number of molecules) contributed to a quarter of the total Raman signal intensity [34]. The highly spatially dispersed accumulation of “hotspots” poses a challenge to the quantitative detection of SERS, making the EF and Raman signal intensity of the noble metal substrate unrepeatable for each detection. Therefore, the development of a SERS substrate with a uniform distribution of “hot spots” is necessary for the quantitative detection of SERS.

3.2. Chemical Enhancement Mechanism

Although the electromagnetic enhancement mechanism can be used to explain most of the SERS phenomena occurring on the surface of noble metal substrates, there are still exceptions [35]. The electromagnetic enhancement mechanism is known to be non-selective, but the Raman signal enhancement of CO and N_2 molecules adsorbed on the surface of the same noble metal substrate

 doi:10.20944/preprints202407.1632.v1

varies widely: the SERS EFs of these two molecules with similar Raman scattering cross sections differ by a factor of 200 under the same experimental conditions. Subsequent studies revealed that the presence of chemisorption between the molecule and the noble metal substrate, or whether the molecule is adsorbed on the substrate active site, is highly dependent on the strength of its Raman signal. These findings suggest that there are other unknown factors that contribute to the enhancement of the Raman signal along with electromagnetic enhancement.

This Raman signal enhancement due to the interaction between the substrate and the probe molecule is called chemical enhancement, and the chemical enhancement mechanism probably includes the following parts [36]. (1) resonance enhancement of the probe molecule, (2) charge transfer resonance enhancement between the probe molecule and the substrate, and (3) non-resonance alteration enhancement (static chemical enhancement of the molecular polarization rate due to adsorption). Among them, the resonance enhancement between the incident light and the probe molecule is independent of the substrate, which is generally categorized into the class of resonance Raman spectroscopy. The SERS EF generated by the resonance between the incident light and the probe molecule usually reaches 103~104 orders of magnitude. In addition, the Raman spectra of probe molecules adsorbed on the substrate surface are different from the Raman spectra of free molecules without adsorption. When the probe molecules are chemically adsorbed on the substrate surface, the interaction between the probe molecules and the substrate or other substances adsorbed on the substrate surface changes the scattering cross-sectional area of probe molecules in the Raman vibrational modes as well as the molecular polarizabilities, which results in the enhancement of the Raman signals [37]. This is the role of chemical enhancement [38–40].

The chemical enhancement effect is now believed to be an independent mechanism that enhances Raman scattering of analytes adsorbed on metal surfaces [41]. The basic elements of chemical enhancement depend on the dependence of the analyte molecule or structure on chemical properties. Electromagnetic enhancement effects are non-selective for chemical properties, while chemical enhancement effects depend entirely on the chemical properties of the molecule itself. For example, differences in enhancement effects of two and more orders of magnitude due to chemical enhancement effects alone can be observed between the CO and N_2 molecules mentioned earlier [42]. In most cases, both electromagnetic and chemical enhancement effects coexist, where electromagnetic enhancement can reach high enhancement effects, while chemical enhancement is usually considered to be less effective than electromagnetic enhancement [43]. Although there is a consensus on the existence of chemical enhancement, the enhancement mechanism remains unclear. For example, experimental observations and theoretical estimates in recent years suggest that the EF of chemical enhancement may be as high as 105-107 [44].

3.3. Theoretical Modeling of SERS Enhancement Effects

With the accumulation of a large amount of experimental data and the continuous progress of numerical processing methods, as well as the development of computer technology in the last decade or so, a solid theoretical and technical foundation has been laid for the systematic study of the relationship between metal nanoparticles and their properties. For the simulation of the SERS effect, various methods have been proposed for numerical processing, such as the method of solving Maxwell's equations, in order to quantitatively calculate the electromagnetic enhancement factor in the SERS system. Currently, there are several numerical treatments for modeling the interaction between material systems and electromagnetic waves, including Finite Difference Time Domain (FDTD), [45–50]. Fourier time domain pseudospectral (Pseudospectral Time-Domain, PSTD), [51,52]. T-array method, [53,54]. Finite Element Method (FEM), Boundary Element Method (BEM), [55–57]. Boundary Element Method (BEM), [58,59]. and Discrete Dipole Approximation (DDA) [60,61]. These numerical methods play an increasingly important role in the fields of electromagnetic wave propagation and scattering, spectroscopy, near-field technology and sensors. Among them, FDTD has been used to successfully calculate and simulate the SERS effect [62–64].

In 1966, Yee [45] first proposed the FDTD numerical algorithm to solve the problem of electromagnetic pulse propagation and reflection in the electromagnetic medium by directly

Preprints.org (www.preprints.org) | NOT PEER-REVIEWED | Posted: 22 July 2024 doi:10.20944/preprints202407.1632.v1

differentiating the system of Maxwell's equations. At first, the electromagnetic field is formed by the alternating propagation of changing magnetic and electric fields, so the value of the electric field at a point in space for a certain period of time depends on the value of the previous period of time at that point and the value of the magnetic field distribution around it, and the corresponding value of the magnetic field is also the same. As shown in Figure 5, four magnetic field components surround one electric field component and four electric field components surround one magnetic field component, so that the electromagnetic field components are sampled in space in a manner that not only conforms to the natural structure of Ampere's Loop Law and Faraday's Law of Electromagnetic Induction, but also conforms to the differential calculation of Maxwell's equations. Thus, given the corresponding initial values of the electromagnetic problem, the electric and magnetic field strengths can be solved step by step by spatial alternation and the spatial electromagnetic field distribution at each moment. The basic idea of the FDTD numerical algorithm is to compute the spatial nodes in the time domain by using the method of the Yee metric, and the nodes of the magnetic and electric fields in the electromagnetic field are discretized by alternating sampling in both time and space, so as to discretize the time domain of the Maxwell's spinodal equations are discretized and transformed into explicit difference equations, and the computational process is greatly simplified. In addition, the FDTD also adopts the computational method of absorbing boundary conditions, which enables the computation to be carried out in a limited spatial range, reduces the complexity of the computational procedure, and reduces the demand for computer hardware.

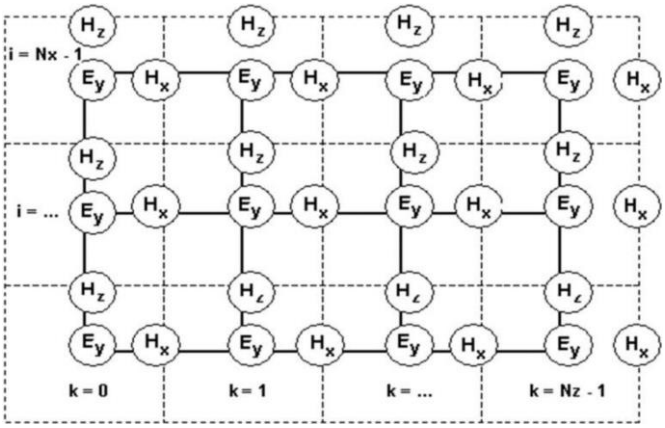

Figure 5. Yee cell distribution in the two-dimensional model [45].

Metallic materials are dispersive materials whose dielectric coefficient changes with frequency. It was not until the 1990s that FDTD began to be applied to this type of material [47]. The material properties of metals are generally treated as modified Debye materials and have their own unique dielectric constants. In FDTD calculations, to ensure the reliability of the material parameters, all parametric calculations need to be fitted directly using the experimentally determined values of the material dielectric coefficients.

3.4. Evaluation of SERS Enhancement Effects

Limit of Detection (LOD) and Raman Enhanced Factor (EF) are two important parameters to evaluate the effect of substrate SERS. However, the calculated value of EF is affected by the Raman detection method, and changes in SERS substrate materials, excitation wavelengths, and probe molecule species all yield different EF values for the calculated results [65]. The EF value can be different from the calculated value. In addition, the estimation method used in the actual calculation process also affects the differences in the calculated EF values. Therefore, depending on the differences in test methods, test conditions and estimation methods, EF can be defined in various ways, such as single-molecule enhancement factor, SERS substrate enhancement factor and analytical enhancement factor [66].

 doi:10.20944/preprints202407.1632.v1

The single molecule enhancement factor is generally used to calculate the Raman signal of a specific molecule, but it is very difficult to calculate the single molecule enhancement factor because the single molecule is very precisely defined and it is difficult to acquire the Raman signal of a single molecule. Therefore, the calculation of single-molecule enhancement factor is only applicable to theoretical estimation for the time being.

Most of the time people are more concerned with calculating the average EF produced by molecules adsorbed on the surface of the SERS substrate rather than calculating the exact Raman signal intensity of each molecule distributed on the surface of the SERS substrate. Therefore, the SERS substrate enhancement factor is usually used to calculate the average Raman enhancement capability of the SERS substrate with the generalized general formula:

$$EF = \frac{I_{surf}/N_{surf}}{I_{bulk}/N_{bulk}},$$

where I_{surf} and I_{bulk} represent the intensities of the same characteristic peaks in SERS and normal Raman detection, respectively, and N_{surf} and N_{bulk} represent the effective number of molecules that can be detected in the Raman laser irradiation area, respectively. If the SERS substrate surface is estimated to be adsorbed as a single molecular layer, the calculation of N_{surf} can be approximated as:

$$N_{surf} = \frac{RA}{\sigma},$$

where R is the roughness factor of the SERS substrate, A is the spot area within the laser irradiation region, and σ is the surface area occupied by adsorbed molecules on the surface of the SERS substrate. The calculation of N_{bulk} has to be based on the confocal characteristics of the system, because the collection efficiency of the scattered photons of the molecules to be measured changes according to the change of the confocal depth. Based on the data of the specific surface area of the substrate and the number of molecules adsorbed on the surface of the substrate, and assuming that the adsorbed molecules are adsorbed in a full monolayer, N_{surf} and N_{bulk} can be calculated by the following equation:

$$N = C \cdot N_A \cdot Sh,$$

where C is the concentration of the probe molecule, N_A represents Avogadro's constant, h is the test focusing depth, and S represents the specific surface area of the SERS substrate S_{surf} , which in conventional Raman measurements represents the laser spot area S_{bulk} . Integration of the above three formulas yields the enhancement factor of the SERS substrate calculated as:

$$EF = \frac{I_{surf}C_{bulk}S_{bulk}}{I_{bulk}C_{surf}S_{surf}},$$

Currently, the way to assess the basal SERS effect using the calculated EF values is still controversial because of the persistent differences between the single-molecule enhancement factor and the SERS basal enhancement factor. Objectively speaking, the calculation of single-molecule enhancement factors is more accurate and reasonable, while the calculation of SERS basal enhancement factors is more practical. Due to the large spatial localization of the "hotspot", the single-molecule enhancement factor varies greatly with the position, so the single-molecule enhancement factor is generally used to accurately analyze the contribution of a single molecule to the Raman enhancement, whereas the SERS base enhancement factor is more practical for analyzing the basal SERS effect, and the SERS base enhancement factor is usually lower than the maximum single-molecule enhancement factor. The SERS base enhancement factor is more practical for analyzing the substrate SERS effect, and the SERS base enhancement factor is usually lower than the maximum single-molecule enhancement factor, so that the substrate SERS effect containing "hot spots" is often underestimated in practical applications. In addition, when the SERS basal enhancement factor is used in practical calculations, it is difficult to obtain the parameter data needed for various calculations precisely, so reasonable estimation assumptions are often given based on the actual test conditions. As a result, the values of SERS basal enhancement factors calculated by

 doi:10.20944/preprints202407.1632.v1

different researchers can vary greatly due to the differences in their respective estimation assumptions or descriptions. This is the current direction for improvement, i.e., a more unified standard is needed to measure the strength of the SERS effect of the substrate.

4. Application of SERS Technology

SERS-based detection technology is a highly efficient and non-destructive trace analysis technique that can detect single molecules or composite molecules. Compared with traditional analytical methods, SERS can accurately identify chemical substances and analyze their structures at the same time [67,68]. SERS has the following characteristics: (1) ultra-high sensitivity, capable of achieving single-molecule detection level; (2) spectral information, which can be used as a "fingerprint" of the molecule; (3) ultra-narrow signal peak bandwidth [69,70]. (3) ultra-narrow peak bandwidth; (4) stability (photodegradation and bleaching resistance); (5) multi-detection function; (6) adjustable substrate structure, which can be used to detect different substances. To date, the application of SERS has expanded from the fields of materials and environmental sciences to biomedicine, involving physical, chemical, and analytical techniques. In recent years, one of the main driving forces behind the progress in SERS research has been the tremendous advancement in nanoparticle preparation technology. SERS substrates are usually composed of nanostructures, and the structure of the nanoparticles can be precisely tuned during the synthesis process, including their size, morphology, and gaps between particles of 2D or 3D nanostructures, which makes the preparation of SERS substrates equally controllable. Based on the precise and controlled preparation of nanoparticles, SERS substrates can be produced quickly, economically, reproducibly and on a large scale for a wide range of applications such as pollutant detection, reactive process detection, biosensing, archaeology and art.

4.1. Food Additives and Pesticide Residues

Food safety has always been closely related to human life, how to accurately detect pesticide residues and food additives is a great concern for countries around the world. Traditional pesticide residue detection methods rely on laboratory sampling, and a series of operations such as sample pretreatment are required before detection. One of the commonly used methods is high performance liquid chromatography (HPLC), which is complex and time-consuming. Therefore, there is an urgent need for a fast and simple method to detect food additives or pesticide residues, and SERS is expected to be utilized for on-site detection of pesticide residues and food additives due to its rapidity and simplicity of the detection process. For example, SERS substrates based on silver nanostructures have successfully detected malachite green (a cancer-causing additive), additives in apple juice and lake water, and mercury ions in river water, among others [71–73]. The preparation of SERS substrates has some problems such as low contact efficiency with the sample under test, low sample collection efficiency, and difficulty in realizing accurate detection. Therefore, the development of flexible SERS substrates is expected to greatly improve the sample collection efficiency and expand its scope. For example, Zhong et al [74]. prepared a flexible SERS substrate with good flexibility, high transparency and strong SERS effect. By self-assembling gold nanoparticles in a polymethylmethacrylate flexible template, a gold nanoparticle/polymethylacrylate film SERS substrate was prepared and used to successfully detect pesticide residues in fish epidermis. Chen et al [75]. prepared a silver-coated carbon nanosphere core-shell structure as a SERS substrate and used the substrate to successfully detect melamine in food.

In addition to the problem of excessive food additives and pesticide residues, there are many harmful substances in the environment that are not conducive to human health, such as organic substances and heavy metal ions. For example, wastewater from industrial production contains a large number of heavy metal ions, such as lead ions, chromium ions and mercury ions, which pose a serious threat to human health and the ecological environment [76]. SERS technology is widely used for in situ detection of pollutants in water bodies due to its advantages of high detection sensitivity, short detection time, low detection cost and low susceptibility to water interference. It should be noted that the elemental valence of chromium has a great relationship with its toxicity. For example,

 doi:10.20944/preprints202407.1632.v1

Cr(VI), the most toxic hexavalent chromium ion, is very easy to accumulate in the human body and cause various diseases. Cr(VI) generally exists in water bodies as the compound CrO_4^{2-} , which is an important indicator of environmental pollution, and therefore a method is needed to rapidly detect Cr(VI) in water bodies. Zhao et al [77]. used TiO_2 nanocolloids sensitized by alizarin red S-sensitization to successfully detect low concentrations of Cr(VI), and the detection limit could reach 0.6 μM, which is lower than the maximum value of Cr(VI) in potable water as stipulated by international regulations. Yu et al [78]. prepared a handheld silicon nano-heterostructure and used it for the simultaneous detection of $Hg2^+$ and $Pb2^+$ in wastewater. The substrate was based on silicon wafers covered with silver nanoparticles, which were also modified with 4-aminothiophenol molecules. The handheld SERS substrate combines sensitivity, selectivity, and convenience to rapidly identify $Hg2^+$ and $Pb2^+$ from ten other interfering metal particles with detection limits of 9.9×10^{-11} M for $Hg2^+$ and 8.4×10^{-10} M for $Pb2^+$, which are two orders of magnitude lower than the U.S. Environmental Protection Agency (EPA) emission standards, and can be used for the practical detection of $Hg2^+$ and $Pb2^+$ in industrial wastewater. Hyanes et al [79]. prepared decanethiol monolayer-modified silver nanoparticles that were successfully used for the detection of PAHs, anthracene and pyrene, as well as other lake swimming pollutants. In order to meet the increasing demand for detection, more types of SERS substrates need to be developed for practical detection.

4.2. Reaction Process Monitoring

Compared with traditional sensing techniques, SERS technology has the capability of non-destructive and real-time in-situ monitoring, so it can be used to monitor the transient intermediates generated in chemical reactions related to non-homogeneous catalysis as well as to analyze the reaction mechanism, which provides an important basis for the optimization of the reaction system. Therefore, SERS technology is also often used to study the process of catalytic reactions. For example, Ding et al [81]. prepared a three-dimensional Fe_3O_4 Au@Ag nanoflower-like structure assembled with nano-chain SERS substrate by in situ reduction and magnetic field-induced assembly. The substrate has high detection sensitivity as well as signal reproducibility, and has been successfully used for nondestructive real-time monitoring of the 4-nitrophenol reduction reaction. As shown in Figure 6 shown, Hu et al [80]. prepared a reaction-mediated SERS nano substrate consisting of newly synthesized gold nanoparticles modified with p-cyclic palladium complexes, which can be used for in situ monitoring of the p-cyclic palladium complex-mediated carbonylation process in a simple and convenient manner without cumbersome pre-treatment. In addition, the kinetic parameters of the reaction can be deduced from the relationship between the reaction time and the ratio of SERS signal intensity at 1319 cm^{-1} and 1338 cm^{-1}. Ouyang et al [82]. prepared a SERS substrate based on Ag nanoparticle-modified HS-β-cyclodextrin Pickering emulsion, which has high SERS activity and is capable of detecting the generation of target compounds as well as monitoring the reaction process, and can also be used for real-time monitoring of the oxidation of o-phenylenediamine for the preparation of 2,3-diaminophenolazine.

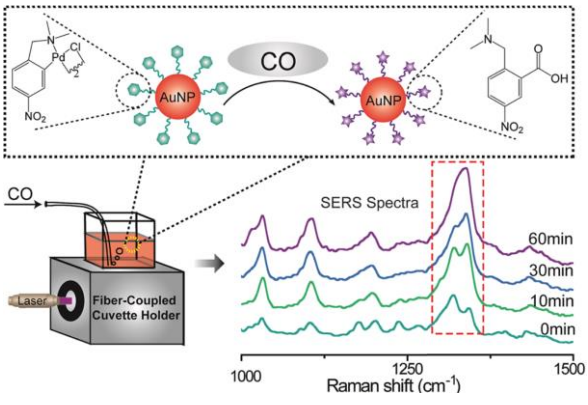

Figure 6. Schematic illustration of the in situ monitoring of palladacycle mediated carbonylation with SERS [80].

 doi:10.20944/preprints202407.1632.v1

4.3. Biomedical Applications

A number of biosensors can be used to detect many biological samples and diseases due to their highly sensitive SERS effect, including a wide range of DNA, viruses, cancers, diabetes, neurological disorders and cardiovascular diseases [34,83–85]. SERS. When analyzing the microenvironment of an organism, the detection of Raman signals is closely related to three parameters [86].: the nature of the substance being analyzed, the nature of the microenvironment within the organism, and the nature of the Raman-enhanced material. In modern medicine, the presence of certain specific molecules in the organism represents the possibility of the occurrence of the relevant disease, and in order to achieve the therapeutic purpose, the parameter level of these specific molecules must be quantified, and then accurate diagnosis can be made to give the appropriate treatment. Currently, although SERS technology can be used for the successful detection of degenerative diseases, such as the detection of amyloid-specific molecules for the diagnosis of Crohn's Felt-Jacob's or Alzheimer's disease, there are still difficulties in the detection of infectious diseases, such as viruses, bacteria, fungi, or other malignant tumors, which do not obviously contain specific molecules. Therefore, it remains a challenge to develop more efficient SERS substrates and assays for the precise and sensitive identification of specific molecules associated with other diseases.

The application of SERS detection technology in biomedicine is categorized into direct and indirect detection, as shown in Figure 7 shown. For biological macromolecules, the use of direct detection is more likely to be interfered by the complex biological microenvironment, while the indirect detection technique can mitigate this interference. Indirect detection requires the preparation of SERS-labeled macromolecules, which are spliced from different functional structures, generally containing a plasma particle, a Raman probe molecule, and a protective shell with a targeting property, and this SERS-labeled macromolecule with targeting property can effectively avoid the interference of other non-specific substances in the biological microenvironment, and improve the specificity of SERS detection.

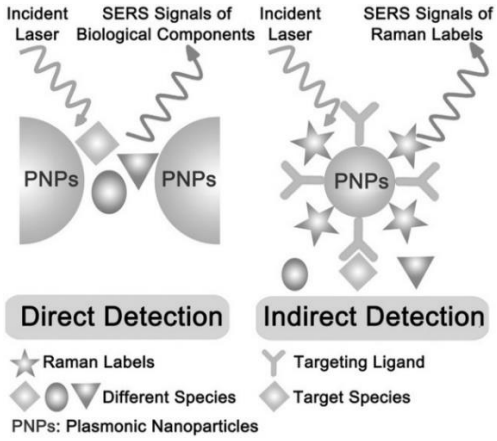

Figure 7. Schematic diagram of direct and indirect detection by SERS technology [87].

Hepatitis B virus (HBV) causes hepatitis B, which is a life-threatening disease. According to the statistics, there are about 350 million HBV carriers in the world, among which there are 3000 deaths every year. HBV carriers are patients who are infected with HBV but do not show symptoms of hepatitis B and have normal liver functions, but nevertheless, HBV carriers can still transmit the virus to other healthy people. Therefore, there is an urgent need to find a simple, rapid, sensitive and reliable HBV test. Conventional HBV assays are based on the measurement of specific light absorbance, while existing assays such as enzyme-linked immunosorbent assay (ELISA) and electrochemical assay (ECA) often require a number of complex intermediate steps, which are time-consuming and expensive. Later, Adem et al [88]. prepared a SERS sensor for the detection of HBV, they connected the DNA molecular strand (which had been labeled with indocyanine green) and the

 doi:10.20944/preprints202407.1632.v1

DNA capture strand on the surface of free gold nanoparticles through HBV DNA, and successfully distinguished and detected the HBV DNA target with the SERS sensor, with the lowest detection limit of 0.44 μM, and also because the gold nanoparticles could be more easily aggregated and thus produce more light absorption rate at about 37 ℃ than at 25 ℃, they were able to detect the HBV DNA target with the SERS sensor. The detection limit of the sensor was further reduced by the fact that gold nanoparticles are more likely to aggregate at around 37 ℃ than at 25 ℃, thus generating a stronger electromagnetic field. This study demonstrates that the ultra-high sensitivity of the SERS sensor has great potential for the selective detection of other unlabeled viruses and proteins. Chourpa et al [89]. used SERS to study the effect of topoisomerase II inhibitors on the corresponding cancer cells and found that topoisomerase II inhibitors could potently inhibit the activity of tumor cells. Cao et al [90]. successfully detected the recognition between immune responses by using SERS and immunization techniques; Zheng et al [91]. obtained the Raman spectrum of chloroferricyclohexine by using SERS. In conclusion, SERS has the advantages of rapidity, simplicity, nondestructiveness, and sensitivity, and has a very good application prospect in biomedicine. It is worth noting that when SERS technology is used in clinical testing, it is usually necessary to take the complex human environment into account, because the serum and plasma of organisms possess a lot of valuable information that can be used for clinical diagnosis, and a large amount of data processing is often required to analyze them, but the SERS substrate can not work in undiluted plasma in a bare manner. To address this difficulty, Sun et al [92]. were the first to synthesize a quasi-3D gold nanostructure array and successfully used it for real-time monitoring of specific drug concentrations in undiluted human plasma. The main design principle is the hierarchical surface modification of the gold nanostructures. First, a layer of self-assembled probe molecules is adsorbed on the surface of the gold nanostructures, and then a layer of amphiphilic polymer brushes is wrapped around them to effectively prevent protein fouling. This SERS substrate has very fast response time and ultra-high sensitivity when used for the testing of target substances. In addition, the SERS substrate can be used to monitor real-time concentrations of several other drugs present in undiluted plasma, such as antidepressants and two other anticonvulsants [93]. The SERS substrate can also be used to monitor real-time concentrations of several other drugs present in undiluted plasma, such as antidepressants and two other anticonvulsants.

Cancer belongs to the most common group of malignant tumors and is a very lethal disease. Governments are committed to taking various measures to prevent deaths caused by cancer. Early means of preventive diagnosis belongs to one of them. Data show that the survival rate of patients diagnosed with cancer at an early stage is higher than that of patients diagnosed at an advanced stage [94,95]. SERS tags are used to capture specific substances of metabolites in serum and analyze their composition to diagnose early cancer development. The specific substances of different metabolites corresponded to different cancers and the time of cancer development. For example, the use of synthesized sea urchin-like gold nanoclusters successfully detected mutated genes occurring in epidermal growth factor [96]. and analyzing the content of specific substances in the exhaled breath to diagnose different stages of gastric cancer by category [97]. etc. Similarly, Cui et al [98]. used a SERS sensor designed to analyze saliva to diagnose and differentiate early or advanced gastric cancer. As shown in Figure 8 shown, the SERS spectra of biospecific substances in four different sets of saliva samples, blank, control, advanced cancer patient, and early cancer patient. By analyzing the biospecific substances in saliva, it is possible to diagnose patients at different cancer stages [99]. This technique has a promising future in clinical applications.

Preprints.org (www.preprints.org) | NOT PEER-REVIEWED | Posted: 22 July 2024 doi:10.20944/preprints202407.1632.v1

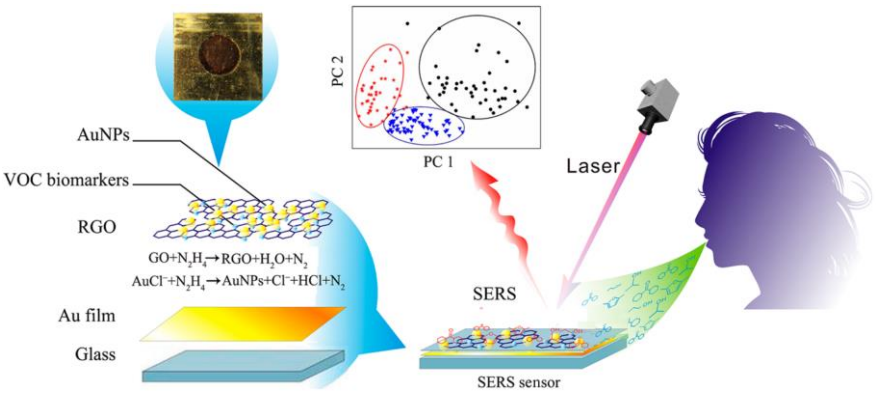

Figure 8. Schematic photographs of breath analysis based on a SERS sensor [98].

Nanomaterial-based SERS technology can also be used for cellular imaging and intracellular drug detection. Raman imaging has higher sensitivity, better recognition ability and anti-interference compared with traditional fluorescent probes, which have contributed to the development of SERS in cellular imaging applications. In 2008, Nie et al [100]. applied SERS imaging technology to in vivo tumor detection for the first time. Since then, SERS imaging has been frequently used in tumor imaging research and applications. In vivo tumor detection usually requires the delivery of SERS probes into the organism and waiting for the SERS probes to be enriched in the tumor tissue before imaging the tumor in vivo. For example, hollow gold nanoparticles can be used to detect marker-specific molecules of human epidermal growth factor cancer, while SiO_2 encapsulated hollow gold nanoparticles are able to detect marker-specific molecules of breast cancer cells and image breast cancer cells, among others. As shown in Figure 9 shown, cellular imaging can be greatly enhanced by detecting specific molecules of cancer cells. In addition, after the cells have absorbed the specific molecules, the detection of these molecules can be used to obtain the location of the cells and the corresponding SERS images [101]. Ren et al [93]. also used 4-mercaptopyridine to modify gold nanoparticles, and then used bovine serum albumin to protect the whole system to prepare SERS probe molecules and successfully monitored the intracellular pH distribution and distribution map.

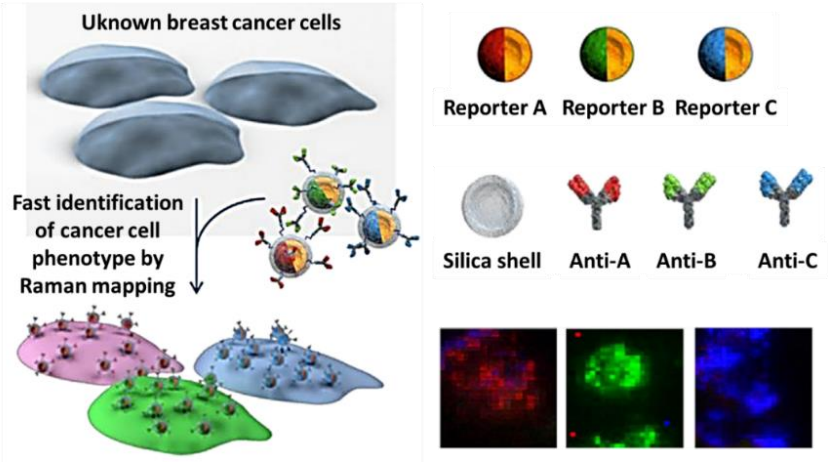

Figure 9. Rapid detection and quantitative evaluation of phenotypic markers on cell surface membranes using the SERS imaging technique [101].

4.4. Archaeology and Art

The SERS technique has been used in the field of cultural and artistic heritage for over thirty years due to its excellent molecular selectivity, ultra-high sensitivity and non-destructive sample detection, especially for the detection and identification of organic colorants such as many natural dyes and some synthetic dyes. The SERS technique has helped to identify many types of organic

 doi:10.20944/preprints202407.1632.v1

colorants from valuable samples of archaeological and artistic significance due to its unique characteristics compared to traditional testing methods. Over the past decade, researchers have recorded the characteristic spectra of different dyes using SERS technology and gradually built up a complete database of dye "fingerprints". Studying the sources of dyes used in the creation of historical artifacts and their possible chemical behaviors during the dyeing process can help archaeological researchers to further unravel the mystery of historical artifacts. Understanding the original shape and color of the artifacts can also help researchers gain a more comprehensive and in-depth understanding of the artist's actual intentions, as well as help them to better distinguish between forged historical artifacts and works of art. Figure 10 is Navajo blanket in the Art Institute of Chicago. SERS spectra of two red fibers in the Navajo blanket were obtained using the SERS technique. [102]. Upon comparative analysis, the spectra were found to be consistent with the SERS spectra of a wool product stained with rouge. In addition to the natural dye carbamic acid detected in the blanket, two organic colorants, cochineal as well as β-naphthol dye, were detected at 785 nm laser. This provides an important reference for accurately deducing when the Navajo blankets were actually manufactured.

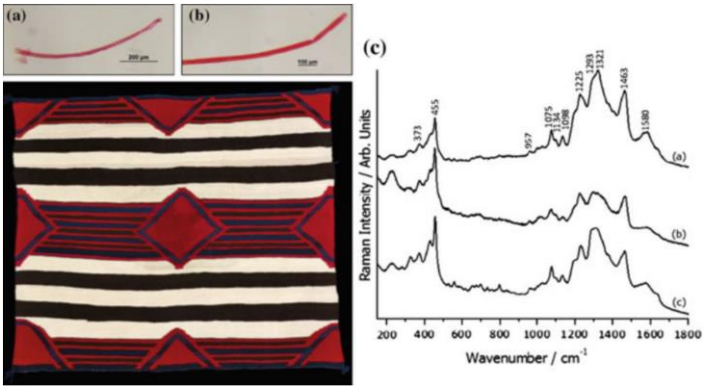

Figure 10. (a, b) The SERS spectra of two red fibers acquired from the Navajo blanket (c) obtained from the wool sample dyed with cochineal [102].

Currently, the SERS technology applied in the field of archaeology and art still faces some challenges, such as the complexity of artifacts and artworks. During SERS testing, various chemicals are adsorbed onto the metal SERS substrate, seriously interfering with the detection of the target dyes. For artifacts with mixed dyes, the metal SERS substrate can often obtain the combined spectra of different dyes at the same time, and the combined spectral peaks are complex and irregular. The spectra of two dyes with disparity in detection limits may also have a covering vs. covered relationship. Therefore, it is very difficult to fully resolve the colorants in the SERS spectra of mixed colorants, and the development of a selective SERS substrate may solve this problem.

Conclusions

The article concludes that SERS is a powerful analytical technique due to its high sensitivity and specificity. The combined understanding of electromagnetic and chemical enhancement mechanisms is crucial for the optimization and practical implementation of SERS technology. Continuous advancements in theoretical modeling and evaluation methods are essential to further enhance the effectiveness of SERS applications in various scientific and industrial fields.

References

1. Smekal, A. Zur quantentheorie der dispersion. *Naturwissenschaften* **1923**, *11*, 873-875.
2. Raman, C. V.; Krishnan, K. S. A new type of secondary radiation. *Nature* **1928**, *121*, 501-502.
3. Settle, F. Handbook of instrumental techniques for analytical chemistry. *Electrical Insulation Magazine IEEE* **1997**, *14*, 42-42.
4. Fredericks, P. M. Infrared and raman spectroscopy in forensic science; John Wiley & Sons, 2012.
5. Willard.; HobartH.; Merritt, L. Instrumental methods of analysis; John Wiley & Sons, 1988.

6. Ewen, S.; Geoffrey, D. Modern raman spectroscopy: A practical approach; John Wiley & Sons, 2004.
7. Willard, H. H.; Merritt Jr, L. L.; Dean, J. A.; Settle Jr, F. A. Instrumental methods of analysis; CBS Publishers & Distributors, 1988.
8. Baena, J. R.; Lendl, B. Raman spectroscopy in chemical bioanalysis. *Current Opinion in Chemical Biology* **2004**, *8*, 534-539.
9. Kudelski, A. Analytical applications of raman spectroscopy. *Talanta* **2008**, *76*, 1-8.
10. Albraheem, L.; Al-Khalifa, H. S. Raman spectroscopy for chemical analysis; John Wiley & Sons, 2000.
11. Sloane, H. J. The technique of raman spectroscopy: A state-of-the-art comparison to infrared. *Applied Spectroscopy* **1971**, *25*, 430-439.
12. Fleischmann, M.; Hendra, P. J.; McQuillan, A. J. Raman spectra of pyridine adsorbed at a silver electrode. *Chemical Physics Letters* **1974**, *26*, 163-166.
13. Jeanmaire, D. L.; Van Duyne, R. P. Surface raman spectroelectrochemistry: Part i. Heterocyclic, aromatic, and aliphatic amines adsorbed on the anodized silver electrode. *Journal of Electroanalytical Chemistry* **1977**, *84*, 1-20.
14. Albrecht M, G.; Creighton J, A. Anomalously intense raman spectra of pyridine at a silver electrode. *Journal of the American Chemical Society* **1977**, *99*, 5215-5217.
15. Tong, L.; Zhu, T.; Liu, Z. Approaching the electromagnetic mechanism of surface-enhanced raman scattering: From self-assembled arrays to individual gold nanoparticles. *Chemical Society Reviews* **2011**, *40*, 1296-1304.
16. Guillot, N.; Chapelle, M. L. The electromagnetic effect in surface enhanced raman scattering: Enhancement optimization using precisely controlled nanostructures. *J Quant Spectrosc Ra* **2012**, *113*, 51-63.
17. Knoll, W. Interfaces and thin films as seen by bound electromagnetic waves. *Annu Rev Phys Chem* **1998**, *49*, 569-638.
18. Moskovits, M. Surface-enhanced raman spectroscopy: A brief retrospective. *Journal of Raman Spectroscopy* **2010**, *36*, 485-496.
19. Moskovits, M.; DiLella , D. P.; Maynard, K. J. Surface raman spectroscopy of a number of cyclic aromatic molecules adsorbed on silver: Selection rules and molecular reorientation. *Langmuir* **1988**, *4*, 67-76.
20. Nitzan, A.; Brus, L. E. Theoretical model for enhanced photochemistry on rough surfaces. *Journal of Chemical Physics* **1981**, *75*, 2205-2214.
21. Garrell, R. L. Surface-enhanced raman spectroscopy. *Annual Review of Analytical Chemistry* **2008**, *1*, 601.
22. Yu, H. K.; Peng, Y.; Yang, Y.; Z.Y., L. Plasmon-enhanced light-matter interactions and applications. *NPJ Computational Materials* **2019**, *5*, 45.
23. Kruszewskh, S.; Skonieczny, J. Roughness effects in surface enhanced raman scattering-evidence for electromagnetic and charge transfer enhancement mechanism. *Acta Physica Polonica* **1991**, *80*, 611-620.
24. Zeman, E. J.; Schatz, G. C. An accurate electromagnetic theory study of surface enhancement factors for silver, gold, copper, lithium, sodium, aluminum, gallium, indium, zinc, and cadmium. *Journal of Physical Chemistry* **1987**, *91*, 634-643.
25. Polavarapu, L.; Liz-Marzán, L. M. Growth and galvanic replacement of silver nanocubes in organic media. *Nanoscale* **2013**, *5*, 4355-4361.
26. Wang, Y. F.; Zhang, J. H.; Jia, H. Y.; Li, M. J.; J.B., Z.; Yang, B.; Zhao, B.; Xu, W. Q.; Lombardi, J. R. Mercaptopyridine surface-functionalized cdte quantum dots with enhanced raman scattering properties. *J Phys Chem C* **2008**, *112*, 996-1000.
27. Shiohara, A.; Wang, Y. S.; Liz-Marzan, L. M. Recent approaches toward creation of hot spots for sers detection. *J Photoch Photobio C* **2014**, *21*, 2-25.
28. Yang, Y.; Li, Z. Y.; Yamaguchi, K.; M., T.; Huang, Z. R.; Jiang, D. L.; Chen, Y. H.; Zhou, F.; Nogami, M. Controlled fabrication of silver nanoneedles array for sers and their application in rapid detection of narcotics. *Nanoscale* **2012**, *4*, 2663-2669.
29. Le Ru, E. C.; Grand, J.; Sow, I.; Somerville, W. R.; Etchegoin, P. G.; Treguer-Delapierre, M.; Charron, G.; Felidj, N.; Levi, G.; Aubard, J. A scheme for detecting every single target molecule with surface-enhanced raman spectroscopy. *Nano Letters* **2011**, *11*, 5013-5021.
30. Hakonen, A.; Svedendahl, M.; Ogier, R.; Yang, Z.-J. Dimer-on-mirror sers substrates with attogram sensitivity fabricated by colloidal lithography. *Nanoscale* **2015**, *7*, 9405-9410.
31. Brus.; Louis. Noble metal nanocrystals:Plasmon electron transfer photochemistry and singlemolecule raman spectroscopy. *Accounts of Chemical Research* **2008**, *41*, 1742-1749.
32. Roy, S.; Muhammed, A. C.; Baik, S.; Kim, J. Silver nanoflowers for single-particle sers with 10 pm sensitivity. *Nanotechnology* **2017**, *28*, 465705.
33. Timur.; Shegai.; Alexan.; Vaskevich; Israel; Rubinstein; Gilad; Haran. Raman spectroelectrochemistry of molecules within individual electromagnetic hot spots. *Journal of the American Chemical Society* **2009**, *131*, 14390-14398.
34. Kleinman, S. L.; Frontiera, R. R.; Henry, A. I.; Dieringer, J. A.; Van Duyne, R. P. Creating, characterizing, and controlling chemistry with sers hot spots. *Physical Chemistry Chemical Physics* **2013**, *15*, 21-36.

 doi:10.20944/preprints202407.1632.v1

35. Metiu, H. Surface enhanced spectroscopy. *Progress in Surface Science* **1984**, *17*, 153-320.
36. Valley, N.; Greeneltch, N.; Van Duyne, R. P.; Schatz, G., C. A look at the origin and magnitude of the chemical contribution to the enhancement mechanism of surface-enhanced raman spectroscopy (sers): Theory and experiment. *J Phys Chem Lett* **2013**, *4*, 2599-2604.
37. Saikin, S. K.; Olivares-Amaya, R.; Rappoport, D.; Stopa, M.; Aspuru-Guzik, A. On the chemical bonding effects in the raman response: Benzenethiol adsorbed on silver clusters. *Physical Chemistry Chemical Physics* **2009**, *11*, 9401-9411.
38. Kneipp, K.; Kneipp, H.; Itzkan, I.; Dasari, R. R.; Feld, M. S. Ultrasensitive chemical analysis by raman spectroscopy. *Chemical Reviews* **1999**, *99*, 2957-2976.
39. Dresselhaus, M. S.; Avouris, P. Introduction to carbon materials research. *Top Appl Phys* **2001**, *80*, 1-9.
40. Cronin, S. B.; Swan, A. K.; Unlu, M. S.; Goldberg, B. B.; Dresselhaus, M. S.; Tinkham, M. Measuring the uniaxial strain of individual single-wall carbon nanotubes: Resonance raman spectra of atomic-force-microscope modified single-wall nanotubes. *Physical Review Letters* **2004**, *93*, 167401.
41. Otto, A. The 'chemical' (electronic) contribution to surface-enhanced raman scattering. *Journal of Raman Spectroscopy* **2005**, *36*, 497-509.
42. Campion, A.; Kambhampati, P. Surface-enhanced raman scattering. *Chemical Society Reviews* **1998**, *27*, 241-250.
43. Campion, A.; Ivanecky III, J. E.; Child, C. M.; Foster, M. On the mechanism of chemical enhancement in surface-enhanced raman scattering. *Journal of the American Chemical Society* **1995**, *117*, 11807-11808.
44. Zhao, L. L.; Jensen, L.; Schatz George, C. Surface-enhanced raman scattering of pyrazine at the junction between two ag_20 nanoclusters. *Nano Letters* **2006**, *6*, 1229-1234.
45. Yee, K. Numerical solution of initial boundary value problems involving maxwell's equations in isotropic media. *IEEE Transactions on Antennas* **1966**, *14*, 302-307.
46. Kunz, K. S.; Luebbers, R. J. The finite difference time domain method for electromagnetics; CRC Press, 1993.
47. Krug, J. T.; Sanchez, E. J.; Xie, X. S. Design of near-field optical probes with optimal field enhancement by finite difference time domain electromagnetic simulation. *Journal of Chemical Physics* **2002**, *116*, 10895-10901.
48. Sullivan, D. M. Electromagnetic simulation using the fdtd method; John Wiley & Sons, 2013.
49. Futamata, M.; Maruyama, Y.; Ishikawa, M. Local electric field and scattering cross section of ag nanoparticles under surface plasmon resonance by finite difference time domain method. *J Phys Chem B* **2003**, *107*, 7607-7617.
50. Futamata, M.; Maruyama, Y.; Ishikawa, M. Microscopic morphology and sers activity of ag colloidal particles. *Vib Spectrosc* **2002**, *30*, 17-23.
51. Liu, Q. H. The pstd algorithm: A time-domain method requiring only two cells per wavelength. *Microwave and Optical Technology Letters* **1997**, *15*, 158-165.
52. Liu, Q. H. Pml and pstd algorithm for arbitrary lossy anisotropic media. *IEEE Microwave and Guided Wave Letters* **1999**, *9*, 48-50.
53. Mishchenko, M. Light scattering by randomly oriented axially symmetric particles. *Journal of the Optical Society of America A* **1991**, *8*, 871-882.
54. Mishchenko, M. I.; Travis, L. D.; Mackowski, D. W. T-matrix computations of light scattering by nonspherical particles: A review. *J Quant Spectrosc Ra* **1996**, *55*, 535-575.
55. Kottmann, J. P.; Martin, O. J.; Smith, D. R.; Schultz, S. Plasmon resonances of silver nanowires with a nonregular cross section. *Physical Review B* **2001**, *64*, 235402.
56. Micic, M.; Klymyshyn, N.; Suh, Y. D.; Lu, H. P. Finite element method simulation of the field distribution for afm tip-enhanced surface-enhanced raman scanning microscopy. *J Phys Chem B* **2003**, *107*, 1574-1584.
57. Kottmann, J. P.; Martin, O. J. F.; Smith, D. R.; Schultz, S. Dramatic localized electromagnetic enhancement in plasmon resonant nanowires. *Chemical Physics Letters* **2001**, *341*, 1-6.
58. Klein, S.; Geshev, P.; Witting, T.; Dickmann, K.; Hietschold, M. Enhanced raman scattering in the near field of a scanning tunneling tip-an approach to single molecule raman spectroscopy. *Electrochemistry* **2003**, *71*, 114-116.
59. Demming, F.; Jersch, J.; Dickmann, K.; Geshev, P. I. Calculation of the field enhancement on laser-illuminated scanning probe tips by the boundary element method. *Appl Phys B-Lasers O* **1998**, *66*, 593-598.
60. Hao, E.; Schatz, G. C. Electromagnetic fields around silver nanoparticles and dimers. *Journal of Chemical Physics* **2004**, *120*, 357-366.
61. Yang, W. H.; Schatz, G. C.; Van Duyne, R. P. Discrete dipole approximation for calculating extinction and raman intensities for small particles with arbitrary shapes. *Journal of Chemical Physics* **1995**, *103*, 869-875.
62. Futamata, M.; Maruyama, Y.; Ishikawa, M. Critical importance of the junction in touching ag particles for single molecule sensitivity in sers. *J Mol Struct* **2005**, *735*, 75-84.
63. Oubre, C.; Nordlander, P. Finite-difference time-domain studies of the optical properties of nanoshell dimers. *J Phys Chem B* **2005**, *109*, 10042-10051.
64. Futamata, M.; Maruyama, Y.; Ishikawa, M. Metal nanostructures with single molecule sensitivity in surface enhanced raman scattering. *Vib Spectrosc* **2004**, *35*, 121-129.

65. Lin, X. M.; Cui, Y.; Xu, Y. H.; Ren, B.; Tian, Z. Q. Surface-enhanced raman spectroscopy: Substrate-related issues. *Analytical and Bioanalytical Chemistry* **2009**, *394*, 1729-1745.
66. Leru, E. C.; Blackie, E.; Meyer, M.; Etchegoin, P. G. Surface enhanced raman scattering enhancement factors: A comprehensive study. *J Phys Chem C* **2007**, *111*, 13794-13803.
67. Li, X.; Ye, S.; Luo, X. Sensitive sers detection of mirna via enzyme-free DNA machine signal amplification. *Chemical Communications* **2016**, *52*, 10269-10272.
68. Jiang, C. L.; Liu, R. Y.; Han, G. M.; Zhang, Z. P. A chemically reactive raman probe for ultrasensitively monitoring and imaging the in vivo generation of femtomolar oxidative species as induced by anti-tumor drugs in living cells. *Chemical Communications* **2013**, *49*, 6647-6649.
69. Schlacker, P. Surface-enhanced raman spectroscopy: Concepts and chemical applications. *Angewandte Chemie International Edition* **2014**, *53*, 4756-4795.
70. Huang, Z. C.; Zhang, A. M.; Zhang, Q.; Cui, D. X. Nanomaterial-based sers sensing technology for biomedical application. *J Mater Chem B* **2019**, *7*, 3755-3774.
71. Li, Z.; Jiang, S. Z.; Huo, Y. Y.; T.Y., N.; Liu, A. H.; Zhang, C.; He, Y.; Wang, M. H.; Li, C. H.; Man, B. Y. 3d silver nanoparticles with multilayer graphene oxide as a spacer for surface enhanced raman spectroscopy analysis. *Nanoscale* **2018**, *10*, 5897-5905.
72. Liang, X.; Wang, Y. S.; You, T. T.; Zhang, X.-J.; Yang, N.; Wang, G.-S.; Yin, P.-G. Interfacial synthesis of a three-dimensional hierarchical mos_2-ns@ ag-np nanocomposite as a sers nanosensor for ultrasensitive thiram detection. *Nanoscale* **2017**, *9*, 8879-8888.
73. Chen, S. H.; Liu, D. B.; Wang, Z. H.; X.L., S.; Cui, D.; Chen, X. Picomolar detection of mercuric ions by means of gold-silver core-shell nanorods. *Nanoscale* **2013**, *5*, 6731-6735.
74. Zhong, L. B.; Yin, J.; Zheng, Y. M.; Liu, Q.; Cheng, X. X.; Luo, F. H. Self-assembly of au nanoparticles on pmma template as flexible, transparent, and highly active sers substrates. *Analytical chemistry* **2014**, *86*, 6262-6267.
75. Chen, L. M.; Liu, Y. N. Surface-enhanced raman detection of melamine on silver-nanoparticle-decorated silver/carbon nanospheres: Effect of metal ions. *ACS Applied Materials & Interfaces* **2011**, *3*, 3091-3096.
76. Ma, W.; Sun, M.; Xu, L.; Wang, L.; Kuang, H.; Xu, C. A sers active gold nanostar dimer for mercury ion detection. *Chemical Communications* **2013**, *49*, 4989-4991.
77. Wei, J.; Yue, W.; Tanabe, I.; Han, X.; Zhao, B.; Ozaki, Y. Semiconductor-driven "turn-off" surface-enhanced raman scattering spectroscopy: Application in selective determination of chromium (vi) in water. *Chemical Science* **2015**, *6*, 342-348.
78. Yu, S.; Chen, N.; Su, Y. Y. Silicon nanohybrid-based sers chips armed with an internal standard for broad-range, sensitive and reproducible simultaneous quantification of lead(ii) and mercury(ii) in real systems. *Nanoscale* **2018**, *10*, 4010-4018.
79. Jones, C. L.; Bantz, K. C.; Haynes, C. L. Partition layer-modified substrates for reversible surface-enhanced raman scattering detection of polycyclic aromatic hydrocarbons. *Analytical and Bioanalytical Chemistry* **2009**, *394*, 303-311.
80. Hu, K.; Li, D. W.; Cui, J.; Cao, Y.; Long, Y.-T. In situ monitoring of palladacycle-mediated carbonylation by surface enhanced raman spectroscopy. *RSC Advances* **2015**, *5*, 97734-97737.
81. Ding, Q.; Zhou, H.; Zhang, H.; Zhang, Y.; Wang, G.; Zhao, H. 3d fe_3o_4@au@ag nanoflowers assembled magnetoplasmonic chains for in situ sers monitoring of plasmon-assisted catalytic reactions. *Journal of Materials Chemistry A* **2016**, *4*, 8866-8874.
82. Ouyang, L.; Li, D.; Zhu, L.; Yang, W. A new plasmonic pickering emulsion based sers sensor for in situ reaction monitoring and kinetic study. *Journal of Materials Chemistry C* **2016**, *4*, 736-744.
83. Li, Q.; Parchur, A. K.; Zhou, A. In vitro biomechanical properties, fluorescence imaging, surface-enhanced raman spectroscopy, and photothermal therapy evaluation of luminescent functionalized $camoo_4$: Eu@au hybrid nanorods on human lung adenocarcinoma epithelial cells. *Science and Technology of Advanced Materials* **2016**, *17*, 346-360.
84. Moore, T. J.; Moody, A. S.; Payne, T. D.; Sarabia, G. M.; Daniel, A. R.; Sharma, B. In vitro and in vivo sers biosensing for disease diagnosis. *Biosensors* **2018**, *8*, 46.
85. Haldavnekar, R.; Venkatakrishnan, K.; Tan, B. Non plasmonic semiconductor quantum sers probe as a pathway for in vitro cancer detection. *Nat Commun* **2018**, *9*, 3065.
86. HU, K.; LI, W. D.; Cui, J.; Cao, Y. In situ monitoring of palladacycle-mediated carbonylation by surface enhanced raman spectroscopy. *RSC Advances* **2015**, *5*, 97734-97737.
87. Zheng, X. S.; Chen, Z.; Xiao, M. X.; X., W.; B., R. Raman imaging from microscopy to nanoscopy, and to macroscopy. *Small* **2015**, *11*, 3395-3406.
88. Zengin, A.; Tamer, U.; Caykara, T. Sers detection of hepatitis b virus DNA in a temperature-responsive sandwich-hybridization assay. *Journal of Raman Spectroscopy* **2017**, *48*, 668-672.
89. Chourpa, I.; Morjani, H.; Riou, J. F.; Manfait, M. Intracellular molecular interactions of antitumor drug amsacrine (m-amsa) as revealed by surface-enhanced raman spectroscopy. *FEBS Letters* **1996**, *397*, 61-64.

 doi:10.20944/preprints202407.1632.v1

90. Cao, Y. W.; Jin, R.; Mirkin, C.; Northwestern, U. Nanoparticles with raman spectroscopic fingerprints for DNA and rna detection. *Science* **2002**, *297*, 1536-1540.
91. Zheng, J. W.; Li, X. W.; Xu, H. Y.; Zhou, Y. G.; Gu, R. A. A non-resonance surface-enhanced raman spectroscopic study of hemin on a roughened silver electrode. *Guang Pu Xue Yu Guang Pu Fen Xi* **2003**, *23*, 294-296.
92. Fang, S.; Hung, H. C.; Sinclair, A.; Z., P.; Tao, B.; Galvan, D. D.; Jain, P.; Li, B.; Jiang, S.; Yu, Q. Hierarchical zwitterionic modification of a sers substrate enables real-time drug monitoring in blood plasma. *Nat Commun* **2016**, *7*, 13437.
93. Zheng, X. S.; Hu, P.; Cui, Y.; Zong, C.; Feng, J.-M.; Wang, X.; Ren, B. Bsa-coated nanoparticles for improved sers-based intracellular ph sensing. *Analytical chemistry* **2014**, *86*, 12250-12257.
94. Torre, L. A.; Bray, F.; Siegel, R. L.; Ferlay, J.; Lortet-Tieulent, J.; Jemal, A. Global cancer statistics. *CA-A Cancer Journal for Clinicians* **2015**, *65*, 87-108.
95. Yazici, O.; Sendur, M. A.; Ozdemir, N.; Aksoy, S. Targeted therapies in gastric cancer and future perspectives. *World Journal of Gastroenterology* **2016**, *22*, 471-489.
96. Wang, L.; Guo, T.; Lu, Q.; Yan, X.; Zhong, D.; Zhang, Z.; Ni, Y.; Han, Y.; Cui, D.; Li, X.; Huang, L. Sea-urchin-like au nanocluster with surface-enhanced raman scattering in detecting epidermal growth factor receptor (egfr) mutation status of malignant pleural effusion. *ACS Applied Materials & Interfaces* **2015**, *7*, 359-369.
97. Hakim, M.; Broza, Y. Y.; Barash, O.; Peled, N.; Phillips, M.; Amann, A.; Haick, H. Volatile organic compounds of lung cancer and possible biochemical pathways. *Chemical Reviews* **2012**, *112*, 5949-5966.
98. Chen, Y. S.; Zhang, Y. X.; Pan, F.; Liu, J. Breath analysis based on surface-enhanced raman scattering sensors distinguishes early and advanced gastric cancer patients from healthy persons. *ACS Nano* **2016**, *10*, 8169-8179.
99. Chen, Y.; Zhang, Y.; Fei, P.; Jie, L.; Cui, D. Breath analysis based on surface enhanced raman scattering sensors distinguishes early and advanced gastric cancer patients from healthy persons. *Journal of Biomedical Nanotechnology* **2018**, *10*, 8169.
100. Qian, X. M.; Nie, S. M. Surface-enhanced raman nanoparticles for in-vivo tumor targeting and spectroscopic detection. *AIP Conference Proceedings* **2010**, *1267*, 81-81.
101. Lee, S.; Chon, H.; Lee, J. Y. Rapid and sensitive phenotypic marker detection on breast cancer cells using surface-enhanced raman scattering (sers) imaging-sciencedirect. *Biosensors* **2014**, *51*, 238-243.
102. Pozzi, F.; Zaleski, S.; Casadio, F.; Leona, M.; Duyne, R. Surface-enhanced raman spectroscopy: Using nanoparticles to detect trace amounts of colorants in works of art; Nanoscience and Cultural Heritage, 2016.